Nuclear Engineering and Technology 52 (2020) 1524–1531

Contents lists available at ScienceDirect

Nuclear Engineering and Technology

journal homepage: www.elsevier.com/locate/net

Original Article

A detector system for searching lost γ-ray source

Waseem Khan, Chaohui He*, Yu Cao, Rashid Khan, Weitao Yang

Department of Nuclear Science and Technology, School of Energy and Power Engineering, Xi'an Jiaotong University, Xi'an, 710049, China

ARTICLE INFO

Article history:
Received 2 June 2018
Received in revised form
16 December 2019
Accepted 20 December 2019
Available online 24 December 2019

Keywords:
Geant4
Gamma-ray source
Geiger muller counters

ABSTRACT

The aim of this work is to develop a Geiger-Muller (GM) detector system for robot to look for a radioactive source in case of a nuclear emergency or in a high radiation environment. In order to find a radiation source easily, a detector system, including 3 detectors, was designed to search γ-ray radiation sources autonomously. First, based on GEANT4 simulation, radiation dose rates in 3 Geiger-Muller (GM) counters were simulated at different source-detector distances, distances between detectors and angles. Various sensitivity analyses were performed experimentally to verify the simulated designed detector system. A mono-energetic ^{137}Cs γ-ray source with energy 662 keV and activity of 1.11 GBq was used for the observation. The simulated results were compared with the experimental dose rate values and good agreements were obtained for various cases. Only based on the dose rates in three detectors, the radiation source with a specific source activity and angle was localized in the different location. A method was adopted with the measured dose rates and differences of distances to find the actual location of the lost γ-ray source. The corresponding angles of deviation and detection limits were calculated to determine the sensitivity and abilities of our designed detector system. The proposed system can be used to locate radiation sources in low and high radiation environments.

1. Introduction

Ionizing radiation is extensively used in industry and medicine, however high exposure can produce deterministic and stochastic effects in human's body. If a radiation source is lost, it can potentially be harmful to people, especially those who are looking for it. In order to reduce the potential hazard to people and the environment, robots are used to find out for the lost radiation sources. Robots play an important role in a high radiation environment that is inaccessible or challenging to humans. With the development of the nuclear industry and robot technology, the function of the radiation detection robot was expanded exponentially. Various groups have used different techniques and detector design systems for robot monitoring of radiation levels and the detection of radioactive sources [1–5]. The earliest detector designs were developed for the MoniRobo-A and MoniRobo-B for the detection of radiation intensity, three-dimensional imaging, and temperature-humidity detection, collect radiation samples and detect combustible gases. The dimension of the individual MoniRobo was 1500 mm × 1500 mm x 800 mm and weighed about 600 kg. It was equipped with robots for removing obstacles and grabbing samples. In the case of the Fukushima nuclear reactor explosion, J. Towler [6] used a scintillation type detector with a special algorithm for estimation and detection of the radiation sources. Lin et al. [7] used a Geiger-Muller (GM) counter to evaluate the position and radiation level of radiation sources without an environmental map. In this case, an approach of the artificial potential field was applied to navigate the radiation sources. Hjerpe et al. [8] presented a statistical method for locating lost point sources in the environment. In this method, different geometries were studied for detector and investigated the radioactive source. Wilhelm et al. [9] used MC based simulation software MNCPX to observe the complete radiological survey, and the NASVD method was adapted for estimation of environmental radioactivity. Sharma et al. [10] developed an algorithm to localize a ^{137}Cs source in a three-dimensional domain. The algorithm implemented in MATLAB and used a domain discretization scheme to predict the source position using measurements from different detector positions. Purkait [11] proposed a radiation mapping approach to estimate the radiation dose rates in the Cyclotron machine and its adjoining areas by using a gamma neutron survey meter. Many approaches were reported regarding the location of the source with a single radiation detector [12–15]. However, an additional detector is required for searching the source actual location [16,21]. Howse

* Corresponding author.
E-mail address: hechaohui@xjtu.edu.cn (C. He).

https://doi.org/10.1016/j.net.2019.12.021

et al. [17] used the least-squares estimation algorithms for tracking the actual location of a ^{137}Cs radioactive source. With the variation of four count rates detected in four γ-ray detectors, the source location at each position was searched in 3 min. A simple detector system was developed by Fujimoto [18] for the identification of incident γ-ray direction. In this approach, with the help of external shields, the direction of γ-ray source was determined within .11.1^o in the measurements of 10–20 min. Another approach was proposed by Willis et al. [19] that determine the actual location of γ-ray source with deviation angle 10.35^o in a short time. They used a set of four radiation detectors in a four-quadrant formation to detect and identify the γ-ray sources. However, the detector system used in these studies is extremely costly and typically too heavy to fit on small mobile robots. To improve the radiation detection capability, a new spatial detector system needs to be developed on a small and inexpensive robot that searches for the position of radioactive sources rapidly and accurately.

This paper presents a simple robot with a detector system that was designed to find lost γ-ray sources only based on the dose rates in the three detectors. In order to improve the detection capability, a 3 GM counters based detector system was developed for searching the radiation sources with a small deviation angle. First, the GEANT4 simulation toolkit was used and analyzed for various cases. For verification, experimental measurements were performed and a system based on the dose rates in detectors was developed. This system has the capability to search and monitor the radioactive sources automatically.

2. Methods

2.1. Monte Carlo simulation

To simulate the passage of particles through matter accurately, Geant4 (version 4.9.6 p02) [20,22], a free software package, is used. The Geant4 includes the facility for handling geometry, tracking, detector response, run management visualization, and user interface. It includes simulation of the electromagnetic interaction of charged particles, gamma, and optical photons. To compute the radiation dose values in detectors, the history of each individual primary photon was traced until its energy dissipated in the detectors producing secondary particles. The secondary electrons formed by photon interaction processes were also taken into consideration in the simulation. Energy deposited in the sensitive volume was stored in the variable dose for all histories. The average energy per history was calculated by dividing the dose with the number of events generated, and the resulted quantity was divided by sensitive volume mass. As a result, the absorbed dose per event (μGy) was obtained. The simulated dose was obtained from using

$$\text{Dose}\left(\mu\text{Gy}\right)=\frac{\text{energy deposited by all particles in a sensitive volume}}{\text{number of }\gamma-\text{rays simulated}\times\text{mass of the sensitive volume}} \quad (1)$$

$$\text{Dose}\left(\mu\text{Gy}\right)=\frac{Q}{N\ M} \quad (2)$$

where Q is the energy deposited by all particles in a sensitive volume, N is the number of gamma rays and M is the mass of the sensitive volume.

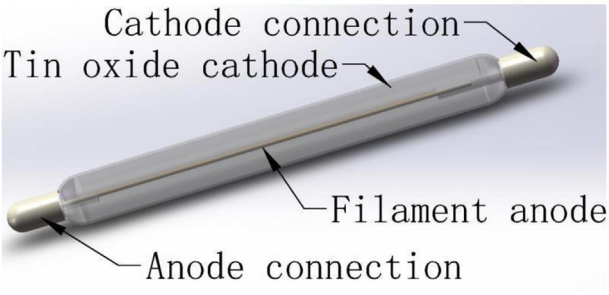

Fig. 1. Schematic of the GM tube.

The dose values were computed by the VMware workstation 15.0.1 software using Intel Quad Core i5 system with build-in 3.6 GHz Processor. The GEANT4 calculation CPU times for dose values, i.e dose values for ^{137}Cs γ-ray energy, were ~0.1 s for the point sources.

The radionuclide simulated for the isotropic point γ-ray source was ^{137}Cs with energy 662 keV and activity of 1.11 GBq. In a single history, a total of 10^7 primary photons was taken for the simulation to obtain a statistical uncertainty of less than 0.5%. The values obtained by the simulation were converted into units of μGy/hr. To get the results in μGy/hr, the following transformations were applied

$$K=\frac{111\times10^7\ \text{Bq}}{10^7}$$
$$=\frac{111\times3600}{\text{hr}}$$

The dose rate was obtained from

$$\text{Dose rate}\left(\frac{\mu\text{Gy}}{\text{hr}}\right)=\frac{Q}{N\ M}\times K \quad (3)$$

Three cylindrical GM detectors were modeled and the simulation was performed in two steps for ^{137}Cs point source. First, the source was fixed and the simulated dose rates were obtained at various locations of the detector system along −Z-axis. In the second case, the dose rates were simulated at different positions of two detectors with ±x-axis and z-axis.

2.2. GM detector design

Due to moderately good gamma discrimination capability and low-cost, GM counter model GMV2 was specially constructed for the experiment with a volume 135 mm × 70 mm × 25 mm and weight about 0.168 kg. The GM tube model J305β was chosen for the radiation sensor board with a cylindrical geometry (length (L) of 100 mm, radius (R) of 10 mm) and its sensitivity γ (^{60}Co) is 65 cps/(μR/s). The GM tube consists of a tin oxide cathode with a coaxial cylindrical thin-walled structure (wall density of 50 ± 10 mg/cm^2) as shown in Fig. 1. The performance specifications of the GM tube are given in Table 1.

Table 1
Performance specifications of the GM tube.

Start count voltage	280–330 V
Recommended operating voltage	380 V
Minimum plateau length	80 V
Maximum plateau slope	10%/80 V
Maximum background count rate	25 times/min
Life	10^9 pulses

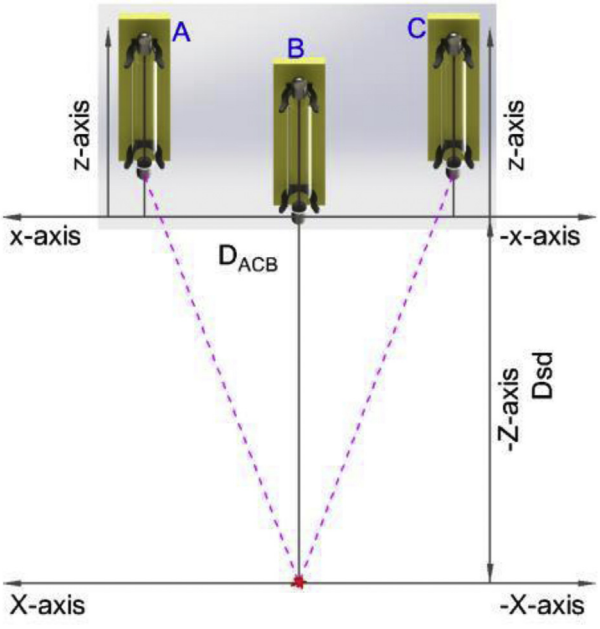

Fig. 2. Designed system for three detectors. Dsd shows the distance between the source and three detectors along −Z-axis, and D_{ACB} is the distance between detectors along ± x-axis and z-axis. ±X-axis is used for deviation away from the axial position.

2.3. Basic mechanism

It is necessary to accomplish a system of multiple detectors to quickly find the actual location of the γ-ray source. For this purpose, we designed a three-detector system. In this system, each detector (GM tube) is labeled as A, B, and C. The relative locations of the detectors and the locations of γ-ray source can be expressed in terms of Cartesian coordinates as shown in Fig. 2. The dose rate in detector B is used to find the distance between the source and system (Dsd) along the -Z-axis and the line between the source and detector B is called the axis. Detectors A and C are on both sides of detector B, used to find the deviation away from the axis. The distance between detector B and detectors A or C is called D_{ACB}, along the ±x-axis and z-axis. The deviation depends on the difference of dose rates in detectors A and C. If the dose rates in detectors A and C are equal then there is no deviation from the axis and the dose rate in detector B only find the Dsd. On the other hand, the difference of dose rates in detectors A and C means the radiation source is not on the axis. In this case, the deviation angle is formed that depends on the difference of dose rates in detectors A and C. The deviation angle increase with the difference of dose rates in both detectors.

2.4. Experimental setup and procedure

The experiment was conducted to verify the simulated results and search the radioactive sources in the real field. The three

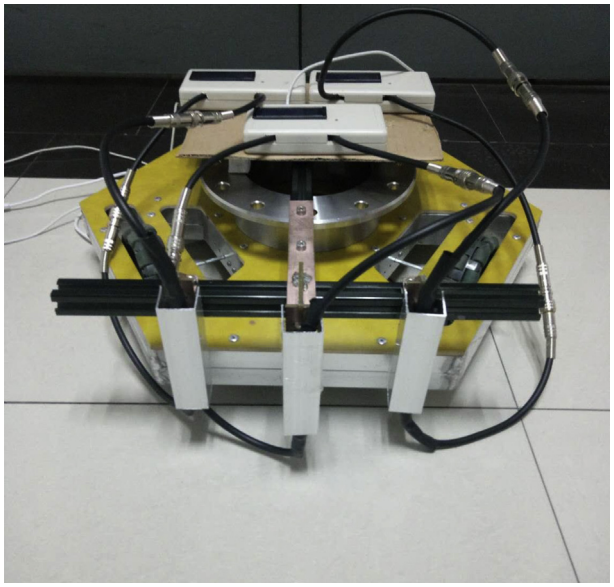

Fig. 3. GM detector system and its connection scheme.

movable GM detectors were connected on a steel metal rod with different distances of the ±x-axis and z-axis. Each detector was inserted in a metal case with a height of 110 mm and a width of 26 mm to avoid the effect of β- and x-rays. A mono-energetic γ-ray source was used with an energy of 662 keV and activity of 1.11 GBq and fixed at a specific position. The lead bricks of length 19 cm, diameter 10 cm, and thickness 3 cm were used around the radioactive source, except for one side. A cart was used to move the detectors system forward, backward and make turning easier. Each GM detector is connected with a cable of approximately 30 cm and each connector linked with the radiation sensor board as shown in Fig. 3. The radiation board consists of two parts, the power circuit, and the signal circuit. The power part is utilized to supply the voltage up to a specific range and the signal circuit is linked with the microcontroller which adjusts the output pulses from the tube. The three radiation sensor boards are connected with the transmitter device (4-port USB 2.0 Ultra-Mini Hub Adapter) to send data to a laptop. When the tube is powered then we received the data on the laptop and count them. For an easy calculation, we can get the value of radiation by Serial Port Utility software. The counting time for each detector was 5 min (can be adjusted) and a total of 60 counts were collected in c/s or μR/hr during this time. Averaged the whole counts and multiplied it by 9.999×10^{-3} to get the dose rate in μGy/hr. The counting dead times were always less than 3% and consequently corrected during the counting. Initially, the experiment was performed to measure the background radiation. The background radiation dose rates in three detectors were 0.30 μGy/h with a relative statistical error (±0.0021 μGy/h). The background subtraction was not included in the measurement. When searching the radioactive sources in an area with stable and low background, there is no need for correction, the actual measured data is enough to find the result.

The standard error (SE) of measurement was calculated using the following equation:

$$SE = \frac{s}{\sqrt{N}} \tag{4}$$

where s is the standard deviation and N is the total number of counts for each detector in different cases.

The relative deviation (RD) between the simulated and the

experimental dose rate values are given by

$$RD = \frac{\text{Experimental Dose rate} - \text{Simulated Dose rate}}{\text{Experimental Dose rate}} \times 100\% \quad (5)$$

3. Results and discussion

3.1. Dose rates in detectors at different source-detector distances (Dsd)

The simulation was performed for different distances between source and detectors (200 cm, 300 cm, 500 cm, and 1000 cm) along the −Z-axis. The distance was fixed from detector B to detector A and C (±6 cm and 1.6 cm) along the ±x-axis and z-axis respectively. The dose rate in detector B was greater than that in detectors A and C because detector B was closer to the γ-ray source. The dose rates were the same in detectors A and C because detectors A and C were placed at the same distance from the detector B. When the Dsd increases, the dose rates of three detectors decrease. Meanwhile, we obtained the dose rates in three detectors experimentally with standard error (vertical bar).

Fig. 4 shows that at the same Dsd, maximum dose rates were observed in three detectors at 200 cm and the dose rates decrease when the detectors move far away from the source. It can be concluded that the dose rates in three detectors depend on the distance between the source and detectors and satisfy the inverse square law theorem. Good agreements were obtained between simulated and experimental results as shown in Fig. 5.

3.2. Dose rates in detectors at different distances between detectors (D_{ACB})

In order to investigate the variation of the dose rates in three detectors with the D_{ACB}, the simulation was performed at fixed Dsd (500 cm) along the -Z-axis for different D_{ACB} ((±4 cm, ±6 cm, and ±8 cm) along ± x-axis and (1 cm, 1.6 cm, and 2 cm) along z-axis). As shown in Fig. 6, at distance (±4 cm along ± x-axis and 1 cm along the z-axis) between detectors in the designed system; the dose rates were higher in two detectors (A and C), because of higher γ-ray photons. At this distance, the detectors A and C were close to detector B, so some scattered γ-ray photons from the metal case

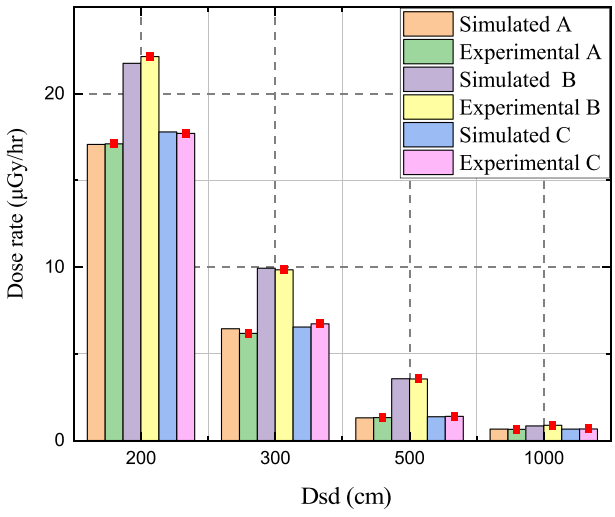

Fig. 4. Comparison of simulated and experimental dose rates at different source–detector distances.

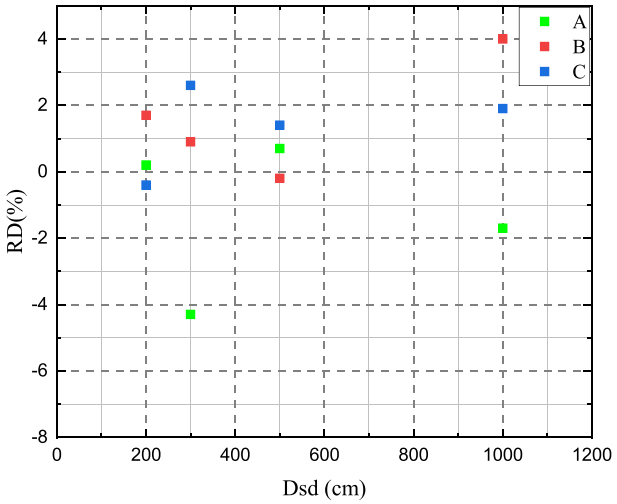

Fig. 5. Relative deviation of the experimental and simulated dose rates at different source-detector distances.

accumulated in detectors A and C. But the dose rate was higher in detector B because detector B was closer to the source than detectors A and C. When the D_{ACB} increased along the ±x-axis and z-axis, the dose rates decreased because as expected the detectors were further away from the source. The γ-rays scattering effect on the dose rates of detectors A and C is not very significant at a greater distance. The detector B was remained fixed during the variation of the position of the detectors; therefore, the dose rate in detector B was observed to stay relatively constant as shown in Fig. 6. Results indicate that a good agreement was achieved between detectors A and C dose rates on D_{ACB} (±6 cm and 1.6 cm). The simulated dose rates agreed with the experimental values within 1.5%, except for the D_{ACB} (±4 cm and ±8 cm) where they are up to 2% and 2.5% respectively as shown in Fig. 7.

3.3. Dose rates in detectors at different angles (θ°)

The detector system was developed to observe the variation of the dose rate at different angles. The radiation source was placed at the fixed position and a distance of 500 cm along -Z-axis from the three detectors. The simulated dose rate was obtained for a fixed D_{ACB} (± 6 cm) along the ± x-axis and (1.6 cm) along the z-axis. Fig. 8 shows that the maximum dose rates were observed in detector B at 0^{o} where the incident γ-rays are in axial position. When the system moves at a distance of 20 cm along -X-axis, then the dose rate in detector A increases, while the dose rates in detectors B and C decrease. At the non-axial position of detectors B and C from the source, a minimum number of γ-rays were deposited in detectors B and C. The detector system was further moved to a distance of 40 cm along -X-axis, the dose rate in detector A consistently increased with the decreasing dose rates in detectors B and C at 4.39^{o}. A good agreement was obtained between the simulated and experimental dose rates with an average relative discrepancy less than 2%. The analysis performed shows that the deviation of angles depends on the dose rate values and increased with the difference of dose rates in detectors A and C. This clearly shows that the sensitivity of the designed system possible at the smallest angles of deviation.

3.4. Interpretation of searching γ-ray source

The experimental results in Fig. 4 show that the dose rates in three detectors were 17.12 ± 0.0111 μGy/h (A), 22.15 ± 0.0120 μGy/h (B) and 17.72 ± 0.0114 μGy/h (C) at Dsd of 200 cm. The different

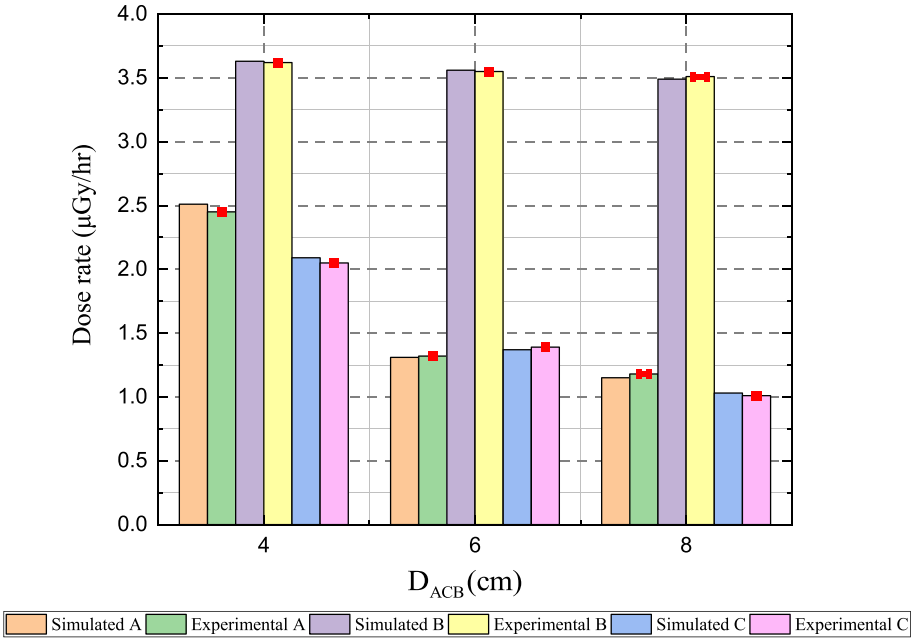

Fig. 6. Simulated and experimental dose rates at different distances between detectors.

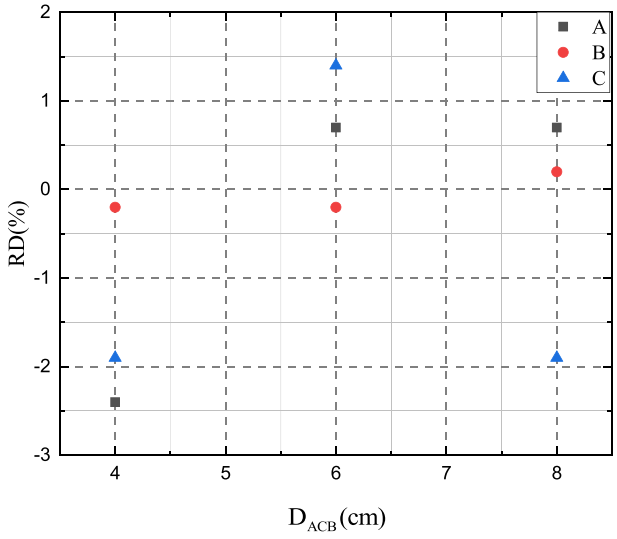

Fig. 7. Relative deviation of dose rates at different distances between detectors.

dose rates in detectors A and C means that the source wasn't on the axis. The dose rate in detector A was smaller than detector C, so the designed system was slightly moved toward the -X-axis. When the dose rate in detectors A and C has become equal, we obtained the distance 1.33 cm along the −X-axis. The dose rate in detector B was used to find the Dsd by using the following equation

$$D = \frac{A\ E\ I}{4\ \pi\ r^2}\frac{\mu_{en}}{\rho} \tag{6}$$

or

$$r^2 = \frac{A\ E\ I\ \mu_{en}}{4\ \pi\ D\ \rho} \tag{7}$$

or

$$r = \sqrt{\frac{A\ E\ I\ \mu_{en}}{4\ \pi\ D\ \rho}} \tag{8}$$

where.

D: dose rate (μGy/hr)
E: energy per decay (keV)
I: γ-ray emission probability (89.9%)
A: activity (GBq) at the time of the measurement
$\frac{\mu_{en}}{\rho}$: mass energy-absorption coefficient of air (29.5 cm^2/kg)

The source was between (200.81 cm (+) and 200.91 cm (−)) along −Z-axis at -X = 1.33 cm. The deviation angle was obtained from

$$\theta = \tan^{-1}\frac{X}{Z} \tag{9}$$

The actual location of the γ-ray source was determined with a deviation angle 0.37^o. The angle was established between detectors B and C. So the actual location of the γ-ray source was closer to detector B because of the higher dose rate.

Using the same methodology, the analyses were examined at different locations (300 cm, 500 cm, and 1000 cm) for searching the γ-ray source. The designed system was displaced along the −X-axis (0.6 cm, 0.2 cm, and 0.4 cm) to obtain the equal dose rates in detectors A and C. The corresponding angle of deviation and the actual locations of the γ-ray source are shown in Fig. 9.

Numerical analyses were carried out based on the measured dose rate values to search the γ-ray source without source activity. The actual location of the lost source was examined based on the dose rates in three detectors at different positions. As shown in Fig. 10, the positions of the designed system from the unknown source are represented by R, S, and T.

Case 1. First, the dose rates in three detectors are noted at S and T positions. The dose rate at S is defined as

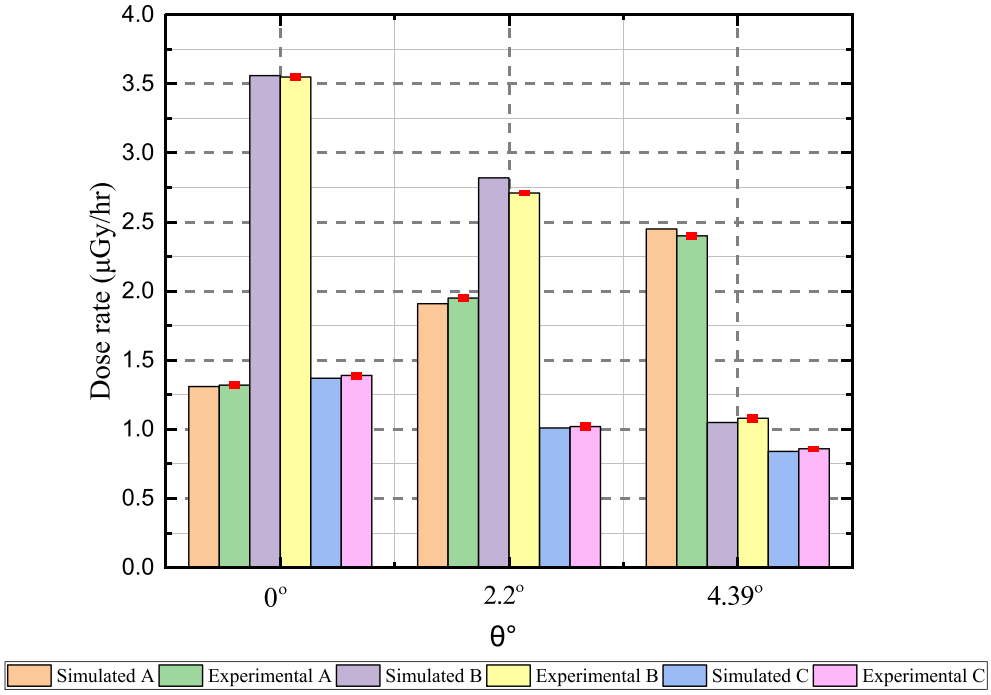

Fig. 8. Comparison of the simulated and experimental dose rates at different angles.

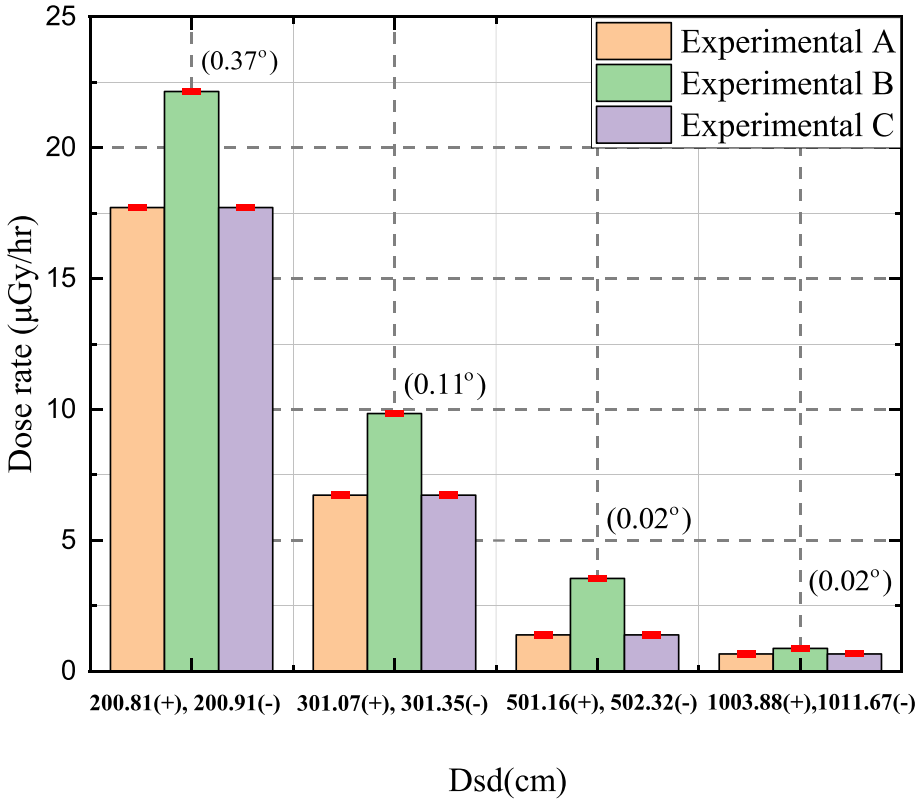

Fig. 9. Results for the actual locations of the γ-ray source at different positions.

$$D_1 = \frac{A\ E\ I}{4\ \pi\ r_1^2}\frac{\mu_{en}}{\rho} \quad (10)$$

The dose rate at T,

$$D_2 = \frac{A\ E\ I}{4\ \pi\ (r_1 - \Delta(^2}\frac{\mu_{en}}{\rho} \quad (11)$$

Solving Eq. (10) and Eq. (11),

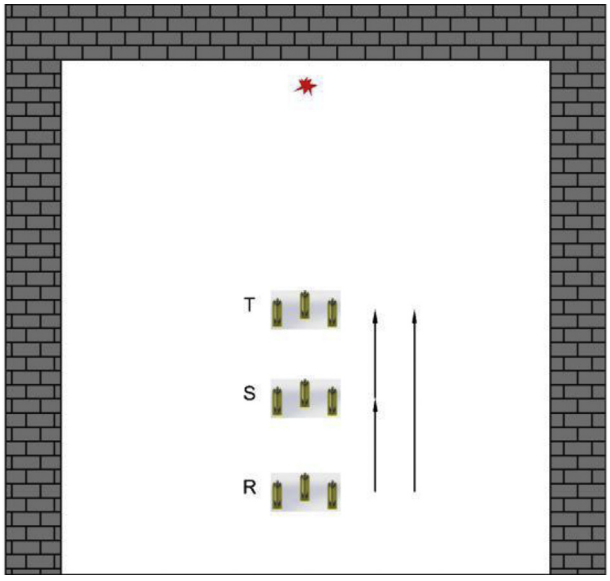

Fig. 10. Searching the lost γ-ray source at different positions (T, S, and R) with the detector system.

$$\left(\frac{D_1}{D_2}-1\right)\ r_1^2+2\Delta r_1-\Delta^2=0 \tag{12}$$

Using the quadratic equation

$$r_{1(+)}=\frac{-\Delta+\Delta\sqrt{\frac{D_1}{D_2}}}{\frac{D_1}{D_2}-1} \tag{13}$$

$$r_{1(-)}=\frac{-\Delta-\Delta\sqrt{\frac{D_1}{D_2}}}{\frac{D_1}{D_2}-1} \tag{14}$$

Both equations are utilized for the actual location of the lost source. Where Δ is the difference of distances.

D_1: Dose rate in detector B at S (9.85 μGy/h)
D_2: Dose rate in detector B at T (22.15 μGy/h)

Based on the dose rate in detector B at two positions, the positions of the lost source were ($r_{1(+)}$ = 60.18 cm and $r_{1(-)}$ = 300.18 cm) using Eq. (13) and Eq. (14) respectively. The difference between the distances of the two positions was 100 cm. For the verification of these results, first the source activities ($A_{(+)}$ = 0.044 GBq and $A_{(-)}$ = 1.110 GBq) were obtained from

$$A_{(\pm)}=\frac{4\ \pi\ r_1^2(\pm)\ \rho\ D_1}{E\ I\ \mu_{en}} \tag{15}$$

For source activity $A_{(+)}$ = 0.044 GBq and distance $r_{1(+)}$ = 60.18 cm, the dose rate ($D_2 = -22.49$ μGy/h), for $A_{(-)}$ = 1.110 GBq, distance $r_{1(-)}$ = 300.18 cm, the dose rate (D_2 = 22.15 μGy/h) were obtained using Eq. (11). The actual location of the lost source was not 60.18 cm because the dose rate should not be negative. A good agreement was observed with the direct measured dose rate in detector B at T position for $r_{1(-)}$ = 300.18 cm. The deviation angle ($\theta^o = 0.11^o$) was obtained from the equal dose rates in detectors A and C at $r_{1(-)}$ = 300.18 cm distance. The actual location of the lost γ-ray source was found at distance 300.18 cm with an angle of deviation 0.11^o.

Case 2. The analysis was carried out for R and S positions. In this case,

D_1: Dose rate in detector B at R (3.55 μGy/h)
D_2: Dose rate in detector B at S (9.85 μGy/h)

The locations of the source were about ($r_{1(+)}$ = 125 cm, $r_{1(-)}$ = 500 cm) with a difference of distances 200 cm. The dose rates at S position were $D_2 = -9.73$ μGy/h and $D_2 = 9.85$ μGy/h with source activities $A_{(+)}$ = 0.068 GBq and $A_{(-)}$ = 1.102 GBq respectively. In this case, the actual location of the lost source was ($r_{1(-)}$ = 500 cm) with deviation angle ($\theta^o = 0.02^o$).

Case 3. The location of the lost γ-ray source was searched with R and T positions.

D_1: Dose rate in detector B at R (3.55 μGy/h)
D_2: Dose rate in detector B at T (22.15 μGy/h)

The positions of the source were ($r_{1(+)}$ = 214.15 cm, $r_{1(-)}$ = 500 cm) with a difference of distances 300 cm. The source activity and dose rate at T position for 214.15 cm ($A_{(+)}$ = 0.202 GBq and $D_2 = -22.06$ μGy/h), and for 500 cm ($A_{(-)}$ = 1.102 GBq and D_2 = 22.15 μGy/h). The actual location of the lost γ-ray source was ($r_{1(-)}$ = 500 cm) with deviation angle ($\theta^o = 0.02^o$). The method we adopted in this report only depends on the dose rates and difference of distances and it is very useful especially for searching the location of the lost γ-ray sources.

The detection limit of the design system (the longest distance from the source that the detectors can detect the radiation) was determined from the background radiation dose rate. The dose rates in three detectors remained same (0.30 μGy/h ± 0.0021 μGy/h) and the longest distance (1719.97 cm (+) and 1732.05 cm (−)) was calculated using Eq. (8). The detection limit depends on the background dose rate and the characteristics of the detector and shows the sensitivity of the designed system.

4. Conclusions

With the increasing risks of nuclear accidents in the nuclear industry, it is important to search the radiation sources for nuclear safety. A special detector system for robot was designed for searching the lost γ-ray source. To determine the sensitivity of the designed system, different analyses of the dose rate with the source-detector distances, distances between detectors and angles were simulated and measured. Experimental measurements were performed and a γ-ray source was localized based on the dose rates in detectors at different positions. Numerical analysis was implemented based on the measured dose rate values for searching the actual location of the lost γ-ray source. The detection limit was calculated based on the radiation background for the sensitivity and ability of our designed system. Results show that the designed system can search the radioactive source quickly and precisely with a small deviation angle. The proposed design system for the robot will play an important role in searching for radioactive materials, radioactive contamination and leakage of radiation.

Declaration of competing interest

The authors declare that they have no known competing financial interests or personal relationships that could have appeared to influence the work reported in this paper.

Acknowledgment

This work at Xi'an Jiaotong University was fully supported by key research and development plan of Shandong Province (Grant No. 2017CXGC0916) and the Chinese government. The authors would like to thank the entire staff of Nuclear Science and Technology Department for providing valuable information in the completion of this work.

Appendix A. Supplementary data

Supplementary data to this article can be found online at https://doi.org/10.1016/j.net.2019.12.021.

References

[1] K. Boudergui, A.M. Frelin, V. Kondrasovs, S. Normand, Integrated sensor handled by robot for dose rate measurement, in: Proceeding of ISOE., 2010.
[2] E. Mishani, N. Lifshits, A. Osavistky, J. Kaufman, N. Ankry, N. Tal, R. Chisin, Radiation levels in cyclotron-radiochemistry facility measured by a novel comprehensive computerized monitoring system, Nucl. Instrum. Methods Phys. Res. A. 425 (1999) 332–342.
[3] S.M. Brennan, A.M. Mielke, D.C. Torney, Radioactive source detection by sensor networks, IEEE Trans. Nucl. Sci. 52 (2005) 813–819.
[4] R. Coulon, J. Dumazert, T. Tith, E. Rohée, K. Boudergui, Large-volume and room-temperature gamma spectrometer for environmental radiation monitoring, Nucl. Eng. Technol. 49 (2017) 1489–1494.
[5] K. Park, J. Kim, K.T. Lim, J. Kim, H. Chang, H. Kim, M. Sharma, G. Cho, Ambient dose equivalent measurement with a CsI (Tl) based electronic personal dosimeter, Nucl. Eng. Technol. 51 (8) (2019) 1991–1997. https://doi.org/10.1016/j.net.2019.06.017.
[6] J. Towler, B. Krawiec, K. Kochersberger, Radiation mapping in post-disaster environments using an autonomous helicopter, Remote Sens. 4 (2012) 1995–2015.
[7] H.-I. Lin, Search strategy of a mobile robot for radiation sources in an unknown environment, in: 2014 International Conference on Advanced Robotics and Intelligent Systems (ARIS), IEEE., 2014, pp. 56–60.
[8] T. Hjerpe, R.R. Finck, C. Samuelsson, Statistical data evaluation in mobile gamma spectrometry: an optimization of on-line search strategies in the scenario of lost point sources, Health Phys. 80 (2001) 563–570.
[9] E. Wilhelm, S. Gutierrez, S. Ménard, A.-M. Nourreddine, Study of different filtering techniques applied to spectra from airborne gamma spectrometry, J. Environ. Radioact. 164 (2016) 268–279.
[10] M.K. Sharma, A.B. Alajo, H.K. Lee, Three-dimensional localization of low activity gamma-ray sources in real-time scenarios, Nucl. Instrum. Methods Phys. Res. A. 813 (2016) 132–138.
[11] M. Purkait, S. Jena, T. Bhaumik, K. Datta, B. Sarkar, C. Datta, D. Sarkar, R. Ravishankar, S.K. Mishra, T. Bandyopadhyay, Online radiation mapping of K-130 Room Temperature Cyclotron using mobile robot, in: Computer and Communication Technology (ICCCT), 2011 2nd International Conference on, IEEE., 2011, pp. 104–107.
[12] A. Miller, R. Machrafi, A. Mohany, Development of a semi-autonomous directional and spectroscopic radiation detection mobile platform, Radiat. Meas. 72 (2015) 53–59.
[13] A.H. Zakaria, Y.M. Mustafah, J. Abdullah, N. Khair, T. Abdullah, Development of autonomous radiation mapping robot, Procedia Comput. Sci. 105 (2017) 81–86.
[14] K. Gamage, M. Joyce, G. Taylor, Investigation of three-dimensional localisation of radioactive sources using a fast organic liquid scintillator detector, Nucl. Instrum. Methods Phys. Res. A. 707 (2013) 123–126.
[15] H.K. Aage, U. Korsbech, Search for lost or orphan radioactive sources based on NaI gamma spectrometry, Appl. Radiat. Isot. 58 (2003) 103–113.
[16] S. Akkoyun, A method for determination of gamma-ray direction in space, Acta Astronaut. 87 (2013) 147–152.
[17] J.W. Howse, L.O. Ticknor, K.R. Muske, Least squares estimation techniques for position tracking of radioactive sources, Automatica 37 (2001) 1727–1737.
[18] K. Fujimoto, A simple gamma ray direction finder, Health Phys. 91 (2006) 29–35.
[19] M.J. Willis, S.E. Skutnik, H.L. Hall, Detection and positioning of radioactive sources using a four-detector response algorithm, Nucl. Instrum. Methods Phys. Res. A. 767 (2014) 445–452.
[20] S. Agostinelli, J. Allison, K.a. Amako, J. Apostolakis, H. Araujo, P. Arce, M. Asai, D. Axen, S. Banerjee, G. Barrand, GEANT4—a simulation toolkit, Nucl. Instrum. Methods Phys. Res. A. 506 (2003) 250–303.
[21] Khan, He, Zhang, et al., Design of CsI (Tl) detector system to search for lost radioactive source, Nuclear Science and Techniques 30(9) (2019) 132, https://doi.org/10.1007/s41365-019-0658-3.
[22] Khan, Zhang, He, et al., Monte Carlo simulation of the full energy peak efficiency of an HPGe detector, Applied Radiation and Isotopes 131 (2018) 67–70, https://doi.org/10.1016/j.apradiso.2017.11.018.